Available online at www.sciencedirect.com
SCIENCE DIRECT®
Pergamon
Cement and Concrete Research 34 (2004) 571–579
CEMENT AND CONCRETE RESEARCH

Experimental investigation and numerical modeling of carbonation process in reinforced concrete structures Part I: Theoretical formulation

Anna V. Saetta[a,*], Renato V. Vitaliani[b]

[a]Department of Architectural Construction, IUAV University of Studies, 30135 Venice, Italy
[b]Department of Structural and Transportation Engineering, University of Padova, 35131 Padua, Italy

Received 5 March 2003; accepted 8 September 2003

Abstract

In this work, the mathematical-numerical model of carbonation process in reinforced concrete (RC) structures, which has been developed by the authors, is applied to different cases of study to take into account the probabilistic nature of durability assessment procedure even if within the framework of a rough and ready approach. In particular, the aim of this Part I of the work is to study how the variability of the parameters defining the differential equations in the model influence the assessment of the corrosion initiation time of RC structure. Comparison with experimental results and numerical simulations are undertaken in Part II of this work.

Keywords: Degradation; Carbonation; Corrosion; Durability; Modeling

1. Introduction

Reinforced concrete (RC) has been a very widely used construction material in civil engineering for many years. We encounter RC structures in our daily lives; the examples of these structures include highway bridges, retaining walls, piers and seawalls, reservoirs and building blocks. Concrete is one of the most versatile, economical and durable construction materials of all time. However, even the most durable concrete can develop cracks and become subject to damage and deterioration due to exposure to salts and carbonation.

Ensuring that RC structures remain safe and in good working condition has become a major concern. Diagnosing deterioration is of fundamental importance for the condition of RC structures to be assessed and for remedial action to be scheduled. The literature reports on a great deal of work that has been done to define methods for predicting the service life of concrete structures (e.g., Refs. [1–13]).

Because an analysis of trends in factors causing the damage of RC structures has shown that corrosion of reinforcement occupy a predominant position, according to the scheme presented by Tuutti [14], we can define the service life T_c for such constructions as the sum of the corrosion initiation time t_0, which is the time it takes for the pollutant to come to coincide with the thickness of the concrete cover, and the corrosion propagation time t_1.

By considering the phenomenon of carbonation, many authors assume that "failure" takes place at the moment when the carbonation front comes into contact with the reinforcement (e.g., Refs. [15–17]), i.e., to identify the "service life" with the "corrosion initiation time." Such a hypothesis disregards the contribution of the corrosion propagation time in the assessment of the service life of the structure, and this can be an oversimplification in some cases, e.g., for internal members of buildings, which can have short initiation time because they are exposed to a dry environment but very long service life because generally there is not enough water in the members to cause steel corrosion. However, the evaluation of the corrosion initiation time provides a useful measure of the structure's durability every time that carbonation phenomenon is activate in external member, because as soon as the carbonation

* Corresponding author.
E-mail address: saetta@iuav.it (A.V. Saetta).

0008-8846/$ – see front matter © 2004 Elsevier Ltd. All rights reserved.
doi:10.1016/j.cemconres.2003.09.009

front has reached the reinforcing bar, the rehabilitation procedure should requires a large amount of time and cost due to the extension of the damage.

In this work, a reliability-based method is proposed to determine the initiation time of reinforcement corrosion in concrete structural members. This method can equip practical engineers with confidence in deciding the maintenance and repairs needed for corroded RC structures.

In particular, the general aim of the present work (Parts I and II) is to establish a protocol for the prognosis of carbonation-induced corrosion and the analysis of degradation for existing and future RC structures. More specific objectives include determining the state of the art as concerns our knowledge of the carbonation-induced corrosion process and inspecting and analyzing some actual RC structures to determine the extent of concrete carbonation and thus provide a reliable estimation of their durability performance in terms of corrosion initiation time.

After a brief outline of the numerical method developed by the authors, this paper presents the study carried out by performing different simulation tests, with the aim of evaluate how the different parameters defining the differential equations in the model influence the assessment of the corrosion initiation time of RC structure.

2. The carbonation process: model-based simulation

A numerical model of deterioration was developed that, providing the details for characterizing the concrete and the environmental conditions are known, offers reliable predictions on the corrosion initiation time of a construction. This model, based on studies by Saetta [5] and Saetta et al. [6,7] and improved with some new features, considers the combination of moisture, heat and pollutant (e.g., CO_2) flows through concrete, including any chemical reactions between cementitious components and the aggressive species.

Assuming that, from experimental results, we know the coefficients of diffusion of water C and of the aggressive substance D_c within the porous matrix of the concrete, the concrete's thermal conductivity b and the other material parameters, the following system of equations can be solved numerically:

$$\text{moisture flow}: \quad \frac{Bh}{Bt} = \operatorname{div}(C\nabla h) + \frac{Bh_s}{Bt} + K\frac{BT}{Bt} + \frac{Bh_c}{Bt} \tag{1}$$

$$\text{heat flow}: \quad \rho C_q \frac{BT}{Bt} = \operatorname{div}(b\nabla T) + \frac{BQ_h}{Bt} + \frac{BQ_c}{Bt} \tag{2}$$

$$\text{pollutant flow}: \quad \frac{Bc}{Bt} = \operatorname{div}(D_c\nabla c) + \frac{c}{\alpha}\frac{Bw}{Bt} + \frac{Bc_c}{Bt} \tag{3}$$

$$\text{rate of chemical reaction}: \frac{B\Re}{Bt} = v = \alpha_4 \times f_1(h) \times f_2(c) \times f_3(\Re) \times f_4(T) \tag{4}$$

where h, T and c are the relative humidity (RH), temperature and concentration of the diffusive species (e.g., carbon dioxide), respectively, and w is the water content. Q_h is the outflow of heat per unit volume of solid and the parameter $\Re$ represents the degree of chemical reaction.

Moreover, $F_1(h)$, $F_2(c)$, $F_3(\Re)$, $F_4(T)$ are functions describing the influence of the presence of water, the concentration of the aggressive species, the degree of chemical reaction and the temperature on the evolution of the chemical process, and the partial derivative with respect to time, i.e., $B(\cdot)_c/Bt$, denotes changes of the parameter in brackets due to chemical reaction per time unit:

$$\frac{Bh_c}{Bt} = \alpha_1\frac{B\Re}{Bt}; \frac{BQ_c}{Bt} = \alpha_2\frac{B\Re}{Bt}; \frac{Bc_c}{Bt} = \alpha_3\frac{B\Re}{Bt} \tag{5}$$

where α_1, α_2, α_3 and α_4 in Eq. (4) are parameters that vary according to the characteristics of the concrete and reagents. A more precise definition of these symbols is given in the previous publications (e.g., Refs. [6,7,15,16]). The influence of the various parameters on the diffusivities can be taken into account by means od a multi-factor law, derived from the one proposed in [17] for humidity diffusion and improved in the subsequent development of the model (e.g., Ref. [18]):

$$C = C_{\text{rif}} F_1^*(h) F_2(T) F_3(t_e) F_4(\Re) \tag{6}$$

$$D_c = D_{c,\text{rif}} F_1(h) F_2(T) F_3(t_e) F_4(\Re) \tag{7}$$

where C_{rif} and $D_{c,\text{rif}}$ are the diffusivities in standard conditions. The F functions, defined in detail in Ref. [18], have the following expressions:

$$F_1^*(h) = \alpha_0 + \frac{1-\alpha_0}{1+\left(\frac{1-h}{1-h_c}\right)^m} \tag{8}$$

$$F_1(h) = (1-h)^{2.5}$$

$$\text{for gas diffusion phenomena (e.g., } CO_2) \tag{9}$$

$$F_1(h) = \left[1+\left(\frac{1-h}{1-h_c}\right)^4\right]^{-1}$$

$$\text{for ion diffusion phenomena (e.g., } Cl^{=}) \tag{10}$$

$$F_2(T) = \exp\left(\frac{Q}{R}\left(\frac{1}{T_0}-\frac{1}{T}\right)\right)$$

$$F_3(t_e) = \chi + (1-\chi)\left(\frac{28}{t_e}\right)^{0.5} \tag{11}$$

For this last relationship, a different value has to be used for the parameter $\chi = D_\infty/D_{28}$, which represents the ratio of the

diffusivity at time = infinity (D_∞) to the diffusivity at time = 28 days (D_{28}) depending on the particular diffusion process.

Finally, if the chemical reaction produces a precipitate, like the calcium carbonate in the carbonation process, for which $\Re=[CaCO_3]/[CaCO_3]_{max}$, the diffusion phenomenon is slowed by the reduction in the porosity and the function $F_4(\Re)$ can be written as, e.g., Refs. [6,7,18]:

$$F_4(\Re) = 1 - \zeta\Re \tag{12}$$

where the parameter ζ varies between 0 and 1.

All the variables should be considered within the framework of a stochastic durability approach because they can vary a great deal locally and may cause considerable scatter. As a consequence, not only average values but also distributions of the variables should be considered. Some preliminary results can be found in [Ref. [21], and this Part I of the work analyzes in detail the influence of the parameters involved in the differential equations used to assess carbonation depth d_c, where the numerical depth corresponds to a degree of chemical reaction $\Re = 0.1$. From the solution of the system of equations, we obtain the time-related trends of the moisture and corrosive substance spreading inside the material and of the degree of the latter's reaction.

It is worth noting that, because the so-called carbonation front is usually defined as a transition zone where the degree of carbonation decreases gradually to zero, in this work, we assume that the carbonation front could be identified by a measure of the parameter "carbonation depth" d_c, as previously defined.

3. Sensitivity analysis

3.1. Mix design

Table 1 provides the essential mix design, and two variations obtained by an increase and a decrease of water content, for a concrete with standard features for use in civil construction work, cast in place in an environment classified as XC3 according to the EN standard 206 [22].

It should be noted that considering a difference in the water content entails changing the water/cement (w/c) ratio, the slump and the compressive strength class (see the tables in the EN standard 206 [22]). Further variations in the parameters that stem from design decisions and the methods used to prepare and cure the concrete were also considered, i.e., more than the water content in the mix (170, 190 or 210 l/m^3), the concrete cover (2, 3 or 4 cm; 3 cm is the minimum concrete cover according to Eurocode 2 [23] plus the tolerance required for cast-in-place structures) and the curing time (24 h, 3 days or 1 week) where curing time is the period of time immediately following placing, when the maintenance of a satisfactory moisture content and temperature in concrete is guaranteed (according to ACI Committee 308-92). The curing conditions are the same in the three cases: with plastic sheets, open treatment, sheltered by rain.

Concerning the system of differential equations (Eqs. (1)–(4)) governing the diffusion and chemical reaction of aggressive substances in concrete, numerical tests were performed to determine the influence of each numerical parameter comprising the input for the model on the final results.

As for the carbonation phenomenon, variations in the depth reached by the carbonation front after 12,000 h (i.e., 500 days) of the onset of the process were taken into account. The previously mentioned mix designs were considered, varying coefficients α_1, α_3, α_4 and the humidity and carbon dioxide transport coefficients. Concerning the carbonation and heat transfer interaction coefficient α_2, different series of analyses have been carried out, the first assuming $\alpha_2 = 0$, to obtain results not influenced from thermal effects, and the others assuming constant values for the parameter α_2. However, due to the lack of experimental data on such an interaction between the heat flow and the chemical reaction producing a inadequate calibration of such an effect, the results illustrated in the paper are those related to the first analysis.

Table 1
Mix design

	Mix design	Variability at +10%	Variability at −10%
Type of cement	Portland	Portland	Portland
Max size aggregate (D_{max}, mm)	20	20	20
Type of aggregate	Rounded	Rounded	Rounded
Slump	(S2)	(S3)	(S1)
Water content (l/m^3)	190	210	170
Cement content (kg/m^3)	380	380	380
w/c	0.5	0.55	0.45
Air content (% vol.)	2	2	2
Concrete	Cast in place	Cast in place	Cast in place
Exposure class	XC3	XC3	XC3
Strength class	(C35/45)	(C30/37)	(C40/50)
Concrete cover (cm)	3	3	3
Finish and state of surface	Standard finish, no cracking	Standard finish, no cracking	Standard finish, no cracking
Curing conditions	3 days of curing with plastic sheet protected from rain	3 days of curing with plastic sheet protected from rain	3 days of curing with plastic sheet protected from rain

3.2. Carbonation and humidity transport interaction coefficient α_1

The coefficient α_1 is related to the maximum content of calcium carbonate $[CaCO_3]_{max} = P_{max}$ (the term P symbolizes the formation of a precipitate), which depends mainly on the concrete's composition and on the angular coefficient of the sorption-desorption isotherm k, dependent basically on temperature, according to a relation of the following kind:

$$\alpha_1 = \frac{PM(H_2O)}{PM(CaCO_3)} k P_{max} = 0.18 k P_{max} \quad (13)$$

Such an equation derives from the kinetic of the carbonation reaction:

$$CO_2 + Ca(OH)_2 \xrightarrow{H_2O} CaCO_3 + H_2O \quad (14)$$

For every $CaCO_3$ molecule produced by the reaction, a H_2O molecule is produced. In terms of molecular mass, we have:

$$M_{H_2O} = M_{CaCO_3} \frac{PM(H_2O)}{PM(CaCO_3)} \quad (15)$$

where M represents the molecular mass of the molecule indicated in subindex and PM(·) represents the molecular weight of the molecule in brackets. As a consequence, in terms of mass per unit volume, Eq. (15) becomes:

$$\frac{M_{H_2O}}{V_{cls}} = \frac{M_{CaCO_3}}{V_{cls}} \frac{PM(H_2O)}{PM(CaCO_3)} \quad (16)$$

where V_{cls} is the considered volume's element. Therefore,

$$dw = dP^* \frac{PM(H_2O)}{PM(CaCO_3)} \quad (17)$$

with dw representing the water content variation per unit volume and unit time, while dP^* is the variation of the calcium carbonate concentration (such variables are both expressed in kg/m^3). By using the well-known expression of the *sorption-desorption* isotherms, i.e., $k dw = dh$, and expressing the calcium carbonate content as $d\Re = dP^*/P_{max}$, we can write:

$$\frac{Bh}{Bt} = \frac{PM(H_2O)}{PM(CaCO_3)} k P_{max} \frac{B\Re}{Bt} \quad (18)$$

which compared with Eq. (5), with $PM(H_2O) = 18.015$ and $PM(CaCO_3) = 100.088$, gives Eq. (13).

Assuming, for instance, that $P_{max} = 0.0096$ kg/m^3 and $k = 1$ m^3/kg, then $\alpha_1 = 0.0017$.

The analytical determination of the coefficient α_1 proves somewhat uncertain because it is difficult to unequivocally assign the coefficients k and P_{max}. These parameters may take on different values as the carbonation process progresses and their value can even vary for concretes with similar compositions.

To assess the influence of the coefficient α_1 on carbonation depth, assuming all other conditions are constant, numerical simulations were performed for the design concrete. Different values of α_1 were used, while all the other parameters were kept constant. The carbonation depth attained 12,000 h after the process had begun was calculated for various RH values assuming the same w/c of 0.5. The obtained values are depicted in Fig. 1 in a-dimensionalized form.

Analyzing these results, we find that the carbonation depth decreases as α_1 increases. As the coefficient α_1 grows, the same mass of water released by the carbonation reaction causes a more evident variation in the RH h and a consequent deceleration in the evaporation phenomenon. Because the CO_2 diffusivity coefficient drops as the value of RH rises, higher α_1 values coincide with lower CO_2 diffusion rates and a consequently more limited penetration of the carbonation front.

It also becomes apparent that the influence of the coefficient α_1 on carbonation depth decreases as the RH increases. In fact, with a rising RH, the gradient of h falls; as a consequence, the concrete drying rate should fall too. In fact, the higher the internal RH, the higher the humidity diffusion coefficient, so the water released by the carbonation reaction has less influence on the rise in internal humidity with rising internal RH values, so that for $h = 1$ its contribution is obviously nil.

Generally speaking, the importance of the coefficient α_1 can be said to decline with increasing water diffusivity values, whatever the reason for them.

The variation in the carbonation depth as a function of the coefficient α_1 is very limited, however, as shown in the graph in Fig. 1. If α_1 is varied between 0 and 1.5, the depth of the carbonation front changes by about 8%, a value comparable with the numerical approximations introduced in the model (estimated to be around 7–7.5% max).

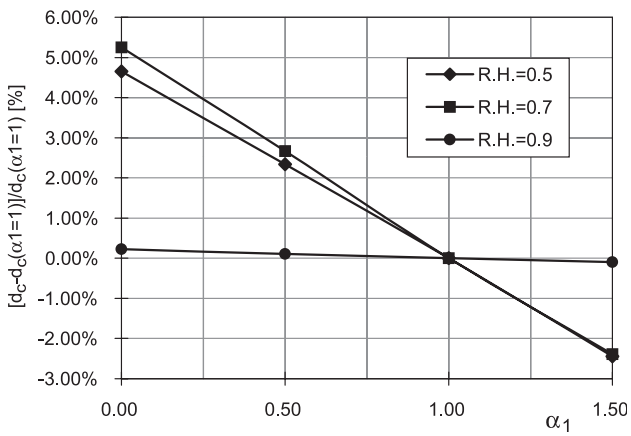

Fig. 1. Percentage influence of the coefficient α_1 on carbonation depth after 12,000 h with different external RH.

3.3. Carbonation and CO_2 diffusion interaction coefficient α_3

Like coefficient α_1, the parameter α_3 also depends on the chemical reaction of carbonation, and based on a few considerations on the chemistry of this reaction, the following relation can be drawn:

$$\alpha_3 = \frac{\mathrm{PM}(\mathrm{CO_2})}{\mathrm{PM}(\mathrm{CaCO_3})}\frac{P_{\max}}{g_{\max}}\frac{g_{\mathrm{env}}}{\beta v} \tag{19}$$

In this case, starting from the carbonation reaction (Eq. (14)), we note that for every $CaCO_3$ molecule produced by the reaction, a CO_2 molecule is consumed. In terms of molecular mass, we have:

$$M_{\mathrm{CO_2}} = M_{\mathrm{CaCO_3}}\frac{\mathrm{PM}(\mathrm{CO_2})}{\mathrm{PM}(\mathrm{CaCO_3})} \tag{20}$$

where the symbols are the same as in Section 3.2. In term of mass per unit volume, Eq. (20) becomes:

$$\frac{M_{\mathrm{CO_2}}}{V_{\mathrm{a}}} = \frac{M_{\mathrm{CaCO_3}}}{V_{\mathrm{a}}}\frac{\mathrm{PM}(\mathrm{CO_2})}{\mathrm{PM}(\mathrm{CaCO_3})} \tag{21}$$

where $V_{\mathrm{a}} = \beta v V_{\mathrm{cls}}$ is the air volume in the considered concrete element V_{cls}, v is the porosity and β is a reducer coefficient (<1), which represents the pores that are not occupied by water. By substituting V_{a} in the right-end side of the previous equation, we have:

$$\mathrm{d}g^* = \mathrm{d}P^*\frac{1}{\beta v}\frac{\mathrm{PM}(\mathrm{CO_2})}{\mathrm{PM}(\mathrm{CaCO_3})} \tag{22}$$

where $\mathrm{d}g^*$ is the variation of CO_2 concentration, while $\mathrm{d}P^*$ is still the variation of the calcium carbonate concentration (such variables are both expressed in kg/m^3). Dividing by $g_{\max}$ (representing the maximum concentration of CO_2 in concrete, expressed in kg/m^3):

$$\frac{\mathrm{d}g^*}{g_{\max}} = \frac{\mathrm{d}P^*}{g_{\max}}\frac{1}{\beta v}\frac{\mathrm{PM}(\mathrm{CO_2})}{\mathrm{PM}(\mathrm{CaCO_3})} \tag{23}$$

Similar to the previous case, using the relation $\mathrm{d}\Re = \mathrm{d}P^*/P_{\max}$, Eq. (23) can be written as:

$$\mathrm{d}\left(\frac{g^*}{g_{\max}}\right) = \mathrm{d}\Re\frac{P_{\max}}{g_{\max}}\frac{1}{\beta v}\frac{\mathrm{PM}(\mathrm{CO_2})}{\mathrm{PM}(\mathrm{CaCO_3})} \tag{24}$$

By assuming a limited variation of the temperature, we can suppose that the density remains constant and the mass concentration be equal to the volume concentration:

$$\frac{c}{g_{\mathrm{env}}} = \frac{g^*}{g_{\max}} \tag{25}$$

where c is the volumetric fraction of the diffusing species CO_2 and g_{env} is the external volumetric fraction. Therefore, Eq. (24) becomes:

$$\frac{B}{Bt}(c/g_{\mathrm{env}}) = \frac{B\Re}{Bt}\frac{P_{\max}}{g_{\max}}\frac{1}{\beta v}\frac{\mathrm{PM}(\mathrm{CO_2})}{\mathrm{PM}(\mathrm{CaCO_3})} \tag{26}$$

which compared with Eq. (5), gives Eq. (19).

For instance, assuming that $P_{\max} = 9.61$ g/m^3, $g_{\max} = 3.60$ g/m^3 and $\beta v = 0.001$ (i.e., that the percentage of air inside the concrete is 0.1% or 1000 cm^3 of air/m^3 of concrete), then:

$$\alpha_3 = 1200 g_{\mathrm{env}} \tag{27}$$

which, for $g_{\mathrm{env}} = 0.035\%$, gives us the value $\alpha_3 = 0.40$.

It is difficult to measure α_3 exactly because it depends on the porosity and internal humidity, which both vary in time, and on the parameters $g_{\max}$ and $P_{\max}$, whose values must be estimated on the basis of the type of concrete.

To determine the influence of the parameter α_3 on the final results, carbonation tests were performed on concrete exposed to an environment with a constant temperature and humidity ($T = 23$ °C, RH $= 0.7$) to assess the depth reached by the carbonation front in the design concrete after 12,000 h, assigning different values to α_3. The results are summarized in Table 2.

The carbonation depth decreases as the coefficient increases because the apparent stoichiometric consumption of CO_2 increases, making it available in smaller and smaller quantities and thus retarding the propagation of the front.

By varying the w/c ratio, the results in terms of percentage carbonation depth (i.e., the carbonation depth d_c referred to the value obtained for $\alpha_3 = 0.5$) versus coefficient α_3 are depicted in Fig. 2. The trend of all the three curves presents two separate areas:

- For small values of α_3, lower than 0.3–0.4 (or for a small $P_{\max}$ with respect to $g_{\max}$), the carbonation reaction uses up a much smaller quantity of CO_2 than is actually available due to the relatively rapid diffusion of the gas in the porous matrix. Therefore, assuming all other conditions as equal, the carbonation phenomenon proceeds very rapidly—governed essentially by the concrete drying out—because the amount of CO_2 available is far greater than the amount consumed in the process. This is the case of cements with a low calcium hydroxide content for which the carbonation phenomenon is not able to modify the pH values of the pore solution. Therefore, the degree of chemical reaction

Table 2
Influence of coefficient α_3 on carbonation depth (mm)

α_3	0.00	0.25	0.50	0.75	1.00
Carbonation depth d_c	18.9736	9.8111	7.8431	6.7857	6.1282

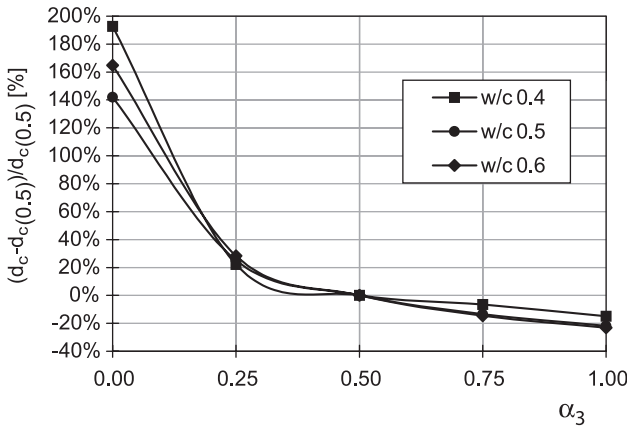

Fig. 2. Percentage influence of the coefficient α_3 on carbonation depth after 12,000 h.

$\Re$ for which we define the numerical depth of carbonation must be greater than 0.1, which is adapted for ordinary cements. Moreover, recent studies assess that "...compared with a plain concrete, the concrete incorporating mineral admixtures (except GGBS with higher fineness and SF) generally showed lower resistance to carbonation possibly due to the dominating effect of the reduction in calcium hydroxide over pore refinement" [24]. Nevertheless, such a problem is still a hot issue in the field of concrete carbonation process.

- For large values of α_3, or P_{max} similar to g_{max}, the curve flattens out, indicating that the progress of the carbonation front is influenced mainly by CO_2 diffusion because the quantity of CO_2 available is of the same order of magnitude as the amount consumed.

For concretes with standard characteristics, like the design mix, α_3 can be assumed to have a value of between 0.4 and 1 (area where the coefficient has the least influence).

3.4. Ideal carbonation rate—coefficient α_4

The coefficient α_4 represents the rate at which the carbonation reaction takes place in ideal conditions, i.e., when all the reducing coefficients in Eq. (4) amount to 1 (degree of carbonation $c=0$, max concentration of CO_2 $g=1$, RH = 90%). If the reaction is rapid, the mass of calcium carbonate produced in a given time interval coincides with the release of a quantity of water that could be more than the porous matrix is capable of expelling in the same time interval, and reaching conditions of equilibrium would slow down the propagation of the carbonation front. Similarly, the quantity of CO_2 consumed during the reaction could be more than the gas that can spread through the concrete in the same time interval, which would again retard the phenomenon. In summary, a higher value of coefficient α_4 corresponds to a state for which the depth of carbonation is lower.

Table 3 shows the results in terms of carbonation depth, demonstrating such a phenomenon: an increasing reaction rate produces a decreasing front propagation rate. In Fig. 3, the effects of different w/c ratios on the relation between the percentage carbonation depth (i.e., the carbonation depth d_c referred to the value obtained for $\alpha_4 = 2.5 \times 10^{-7}\ s^{-1}$) and the coefficient α_4 are shown.

Because the variability of the rate of the carbonation process, where no reaction accelerators are involved, can be assumed to be no more than 10–15%, assuming $\alpha_4 = 2.80 \times 10^{-7}\ s^{-1}$ (obtained from experimental results on standard concrete), the influence of said coefficient on the end result is less than 2% and can thus be deemed negligible.

3.5. Diffusivity of water C and carbon dioxide D_c

The values for the diffusivity of humidity and CO_2 are the parameters that most affect the carbonation phenomenon because the presence of humidity and CO_2 inside the pores is fundamental to the onset and progression of carbonation. Moreover, because both can be brought down more or less directly to the porosity and permeability of the concrete, these diffusivities represent the most significant numerical characterization of the type of cement, the w/c ratio and all the other factors that distinguish one concrete from another.

Judging from the numerical test results, summarized in Tables 4, the depth of carbonation is logically proportional to the diffusivity of both the humidity and the CO_2.

As regards the propagation of humidity, a 25% increase in the diffusivity with respect to the reference value $C_{ref} = 2 \times 10^{-11}\ m^2/s$ of the water coincides with an $\sim$ 2.53% increase in the depth of carbonation. Similar results emerge for a 25% reduction in diffusivity (which induces a 2.88% reduction in the depth of carbonation).

Concerning the diffusion of CO_2, a 25% variation in the value of D_c with respect to the reference value $D_{cref} = 3 \times 10^{-8}\ m^2/s$ leads to a variation in the depth of carbonation of about 9%.

Fig. 4 shows the percentage influence of the variation of diffusivities C and D_c on carbonation depth after 12,000 h for three different w/c ratios.

Table 3
Influence of coefficient α_4 on carbonation depth (mm)

α_4	1.00×10^{-7}	1.50×10^{-7}	2.00×10^{-7}	2.50×10^{-7}	3.00×10^{-7}
Carbonation depth d_c	6.9269	6.6259	6.3860	6.1929	6.0998

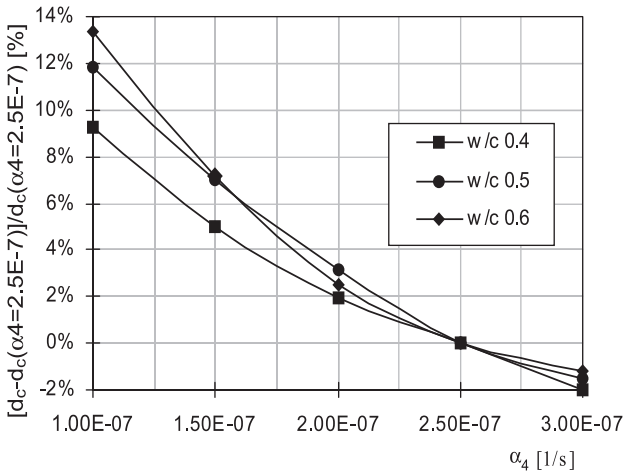

Fig. 3. Percentage influence of the coefficient α_4 on carbonation depth after 12,000 h.

From the numerical standpoint, the two diffusivities come to bear on the carbonation phenomenon in much the same way, although D_c is virtually twice as influential as C, and this means that neither of these two parameters can be considered negligible in relation to the other.

3.6. Cement hydration coefficient $\chi = D_\infty/D_{28}$

The cement hydration coefficient $\chi = D_\infty/D_{28}$ (see Eq. (11)) indirectly influences the depth of carbonation, because it contributes toward determining the variation in the time-related diffusivity of both the humidity and the gas due to progressive hydration.

If $\chi = 1$, the diffusivity does not vary with time because of the curing process (although it does vary for other reasons), while for $\chi < 1$, the variation is all the more accentuated, the smaller the value of χ, as we can see from the trend of the carbonation depth (as a percentage) after 12,000 h as a function of χ shown in Fig. 5.

The influence of χ on carbonation depth is around 7–20% for the values adopted for the design concrete ($\chi = 0.5$–0.8).

3.7. Discussion and results

The various parameters analyzed differ in importance as regards the end result or the depth reached by the carbonation front after a certain time interval.

Table 4
Influence of the diffusivity of humidity C and carbon dioxide D_c on carbonation depth

C (m^2/s)	d_c (mm)	D_c (m^2/s)	d_c (mm)
1.00×10^{-11}	5.7255	1.500×10^{-8}	4.7951
1.50×10^{-11}	5.9440	2.250×10^{-8}	5.6578
2.00×10^{-11}	6.1203	3.000×10^{-8}	6.2818
2.50×10^{-11}	6.2751	3.750×10^{-8}	6.8014
3.00×10^{-11}	6.3805	4.500×10^{-8}	7.2473

Table 5
Concentration of CO_2 measured in different types of environment

No.	Sample from	CO_2 [μV s]	CO_2 concentration [% vol.]
1	Open country	2293	0.015
2	City center	5469	0.036
3	Industrial zone	6814	0.045
4	Well-aired stable	6880	0.046
5	Stable	11,217	0.075
6	Motor car exhaust	2,513,424	16.690
7	Human breath	545,152	3.62

The humidity and CO_2 diffusivity values are unquestionably fundamental, although significant variations in the end results only occur for marked differences in the diffusion coefficients. For these parameters, a probability study is needed to attribute them a statistic based on probabilistic criteria.

The coefficients α_1 and α_4, on the other hand, are less sensitive in that, having adopted a value that guarantees a good consistency with the experimental findings (values of $\alpha_1 = 0.002$ and $\alpha_4 = 2.80 \times 10^{-7}\ s^{-1}$ are recommended for the design concrete with w/c of 0.5), the final results are only mildly influenced by variations in the two coefficients, which can thus be treated as variables of deterministic/experimental type.

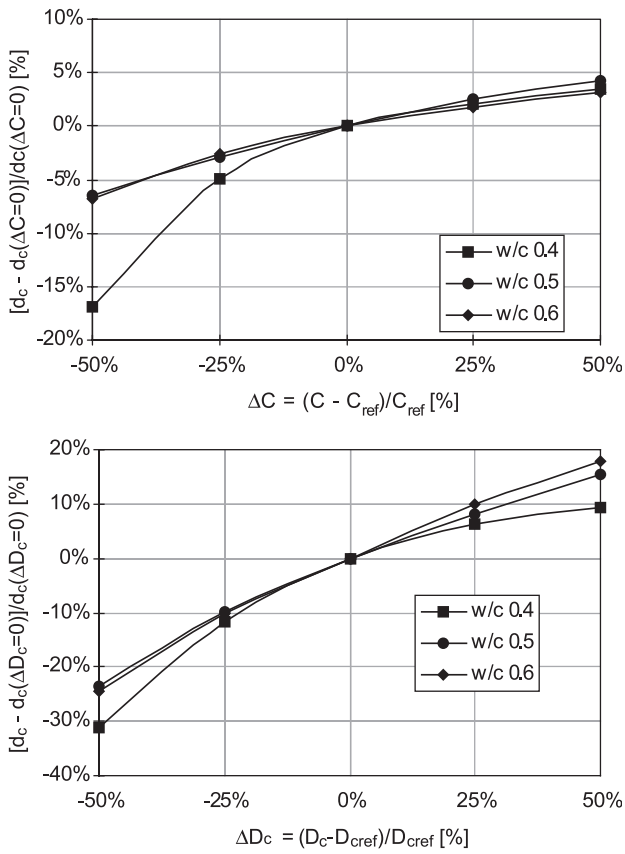

Fig. 4. Percentage influence of the coefficients C and D_c on carbonation depth after 12,000 h.

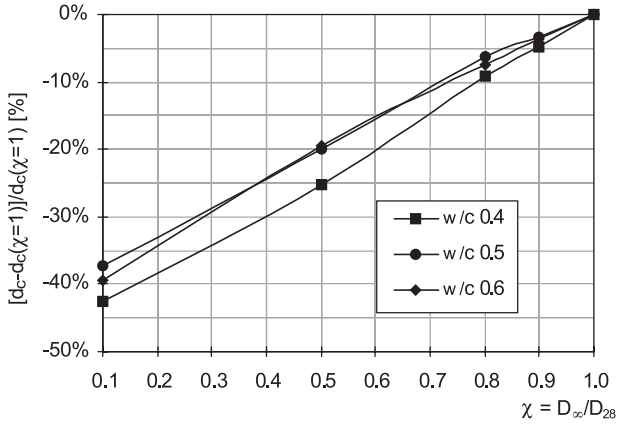

Fig. 5. Percentage influence of $\chi = D_\infty/D_{28}$ on carbonation depth after 12,000 h.

The importance of the parameter α_3 remains uncertain, however. Among the coefficients of interaction between carbonation and other diffusion phenomena, this is the one that presents the greatest variability as the phenomenon evolves. Using Eq. (14) to assess said parameter is a good compromise between simplicity of expression and approximation error. Here, again, a probabilistic study would be useful for this parameter.

Having assessed the influence of the coefficients in the system of Eqs. (1)–(4) on the resulting carbonation depth after 12,000 h, the numerical model is applied to determine the corrosion initiation time of the design concrete, bearing in mind the various cases considered.

For the design concrete, the corrosion initiation time $t_0 = 60$ years.

As a consequence of the predicted variations, the following values are obtained:

1. Variation in water content $\pm$ 10%:
   water +10%: $t_0 = 45$ years
   water −10%: $t_0 = 85$ years

2. Variation in concrete cover:
   Concrete cover 4 cm: $t_0 = 107$ years
   Concrete cover 2 cm: $t_0 = 32$ years

3. Variation in curing time:
   Curing time 1 week: $t_0 = 68$ years
   Curing time 24 h: $t_0 = 46$ years

4. Conclusions

In recent years, increasing attention has been paid to the durability of plain and RC structures. The enormous number of RC structures built in the last few decades and their premature failure and damage have led to increasing costs for their repair, maintenance and restoration, also prompting concern as to the safety of such constructions.

It consequently becomes necessary to ensure a guaranteed adequate service life for RC structures in the design phase. However, the problem of designing RC structures for a given service life or predicting the service life of existing structures can only be overcome by considering the interaction between the structural materials (i.e., concrete and steel) and the environment—a far from simple task that depends heavily on the characteristics of the materials and their environmental conditions.

The model presented here for simulating the carbonation process enables the influence of the various parameters involved to be considered in the governing equations. In particular, a first attempt has been made in this work to investigate the sensitivity of the model to variations in said parameters. The aim was to determine which parameters have to be evaluated using a stochastic approach (said approach will be the object of future studies). In Part II of this paper, some applications are developed for which experimental tests as well as numerical simulations that illustrate the formulation developed herein are presented and discussed in detail. It is worth noting that one of the fundamental environmental parameters that most affects the rate of carbonation, is the concentration of CO_2 in the air. Table 5 gives the CO_2 values measured in different environments, in terms of volumetric concentration, which will be necessary for the applicability of the proposed model.

Acknowledgements

We thank Mauro Bono for his contribution during the preparation of his degree thesis.

Appendix A. List of symbols

The following symbols are used in this paper:

b	heat conductivity
C	relative humidity diffusion coefficient
C_{rif}	relative humidity diffusion coefficient in standard conditions
C_q	isobaric heat capacity
c	total concentration of the diffusive species
d_c	carbonation depth
D_c	aggressive species diffusion coefficient
$D_{c,rif}$	aggressive species diffusion coefficient in standard conditions
D_∞	aggressive species diffusion coefficient at time = infinity
D_{28}	aggressive species diffusion coefficient at time = 28 days
g_{max}	maximum concentration of CO_2 in concrete, expressed in kg/m^3
g_{env}	external volumetric fraction of the diffusing species CO_2
h	relative humidity
h_c	the humidity at which the diffusivity C drops half-way between its maximum and minimum values ($h_c = 0.75$)
h_s	the self-desiccation
K	hygrothermic coefficient
m	the spread of the drop in the diffusivity C, variable between $m = 6$ and $m = 16$

Appendix A (*continued*)

Q	activation energy of the diffusion process
Q_h	outflow of heat per unit volume of solid
P_{max}	maximum content of calcium carbonate
$\Re$	degree of chemical reaction
R	gas constant
T	temperature
T_0	reference temperature (in K, usually 296 K)
T_c	service life
t	time
t_0	corrosion initiation time
t_1	corrosion propagation time
t_e	equivalent curing time
w	water content
α	capacity factor, measure of the binding capacity of the material for a particular diffusant
α_1	parameter that accounts for the possible interaction between the moisture flow and the chemical reaction
α_2	parameter that accounts for the possible interaction between the heat flow and the chemical reaction
α_3	parameter that accounts for the possible interaction between the pollutant flow and the chemical reaction
α_4	parameter that accounts for the dependence of the rate of reaction on the concrete characteristics
α_o	the ratio min C/max C, ranging between 0.025 and 0.10
χ	ratio between the diffusion coefficient for $t_e \rightarrow \infty$ and the diffusion coefficient for $t_e = 28$ days
ζ	parameter varying between 0 and 1, which measures the slowing of diffusion phenomenon due to reduction of the porosity

References

[1] RILEM Seminar on the Durability of Concrete Structures Under Normal Outdoor Exposure, March 26–29, Hannover, pp. 182–196, 1984.

[2] D.W.S. Ho, R.K. Lewis, Carbonation of concrete and its prediction, Cem. Concr. Res. 17 (1987) 489–504.

[3] Y. Houst, F.H. Wittmann, Diffusion de gaz et durabilité du béton armé, IABSE Symposium, Durability of Structures, Lisbon, 1989, pp. 139–144.

[4] R.J. Clifton, Predicting the service life of concrete, ACI Mater. J. 90 (6) (1993) 611–617.

[5] A. Saetta, Durabilità delle strutture di calcestruzzo armato e analisi dei fenomeni di diffusione dei materiali multifase, PhD dissertation, Padova, 1992.

[6] A.V. Saetta, B.A. Schrefler, R.V. Vitaliani, The carbonation of concrete and the mechanism of moisture, heat and carbon dioxide flow through porous materials, Cem. Concr. Res. 23 (4) (1993) 761–772.

[7] A.V. Saetta, B.A. Schrefler, R.V. Vitaliani, 2-D Model for carbonation and moisture-heat flow in porous materials, Cem. Concr. Res. 25 (8) (1995) 1703–1712.

[8] N.R. Buenfeld, N.M. Hassanein, Life prediction of concrete structures using neural networks, Proc. Inst. Civ. Eng. Struct. Build. 128 (1998) 38–48.

[9] M.T. Liang, K.L. Wang, C.H. Liang, Service life prediction of reinforced concrete structures, Cem. Concr. Res. 29 (9) (1999) 1411–1418.

[10] T.J. Kirkpatrick, R.E. Weyers, M.M. Sprinkel, C.M. Anderson-Cook, Impact of specification changes on chloride-induced corrosion service life of bridge decks, Cem. Concr. Res. 32 (8) (2002) 1189–1197.

[11] B. Zuber, J. Marchand, Modeling the deterioration of hydrated cement systems exposed to frost action—Part 1. Description of the mathematical model, Cem. Concr. Res. 30 (12) (2000) 1929–1939 (Special Issue).

[12] E.J. Hansen, V.E. Saouma, Numerical simulation of reinforced concrete deterioration—Part I: Chloride diffusion, ACI Mater. J. 96 (2) (1999) 173–180.

[13] A. Steffens, D. Dinkler, H. Ahrens, Modeling carbonation for corrosion risk prediction of concrete structures, Cem. Concr. Res. 32 (6) (2002) 935–941.

[14] K. Tuutti, Corrosion of steel in concrete, Swed. Cem. Concr. Res. Inst. 1 (1982) 17.

[15] Y.F. Houst, P.E. Roelfstra, F.H. Wittmann, A model to predict service life of concrete structures, in: F.H. Wittman (Ed.), Proc. International Colloquium on Material Science and Restoration, Edition Lack und Chemie-Verlag, Filderstadt, 1983, pp. 181–186.

[16] S. Rostasy, D. Bunte, Evaluation of on-site conditions and durability of concrete panels exposed to weather, IABSE Symposium, Lisbon, in: IABSE-AIPC-IVBH ETH Hönggerberg-Zürich. 57 (1989) pp. 145–149

[17] Z. Keršner, B. Teplý, D. Novák, Uncertainty in service life prediction based on carbonation of concrete, in: C. Sjöström (Ed.), Durability of Building Materials and Components, 7DBMC, Stockholm, Sweden, E&FN Spon, NY, USA, 1996 (May).

[18] A. Saetta, R. Scotta, R. Vitaliani, Mechanical behaviour of concrete under physical-chemical attacks, J. Eng. Mech. ASCE 124 (10) (1998) 1100–1109.

[19] A. Saetta, R. Scotta, R. Vitaliani, Reliability of reinforced concrete structures under chemical-physical attack, invited paper, AJSE 23:2C (1998), Theme Issue Concrete Repair, Rehabilitation and Protection.

[20] Z.P. Bažant, L.J. Najjar, Nonlinear water diffusion in nonsaturated concrete, Mater. Struct. (RILEM, Paris) 5 (25) (1972) 3–20.

[21] Saetta, A., Analisi di sensibilità dei modelli di previsione del degrado delle strutture di calcestruzzo armato (in Italian), Giornale del Genio Civile, fasc. 10°-11°-12° (1996) 224–240.

[22] COMITE EUROPEEN DE NORMALISATION, EN 206-1 " Concrete—Part 1: Specification, performance, production and conformity," September 2000.

[23] UNI ENV 1992-1-1—31/01/1993—Eurocodice 2. Progettazione delle strutture di calcestruzzo. Parte 1-1: Regole generali e regole per gli edifici.

[24] P. Sulapha, S.F. Wong, T.H. Wee, S. Swaddiwudhipong, Carbonation of concrete containing mineral admixtures, J. Mater. Civ. Eng. 15 (2) (2003 Mar.–Apr.) 134–143.